



CHORUS

This is the accepted manuscript made available via CHORUS. The article has been published as:

Optical Absorption in Degenerately Doped Semiconductors: Mott Transition or Mahan Excitons?

André Schleife, Claudia Rödl, Frank Fuchs, Karsten Hannewald, and Friedhelm Bechstedt

Phys. Rev. Lett. **107**, 236405 — Published 30 November 2011

DOI: [10.1103/PhysRevLett.107.236405](https://doi.org/10.1103/PhysRevLett.107.236405)

Optical absorption in degenerately doped semiconductors: Mott transition or Mahan excitons?

André Schleife,^{1,2,3,*} Claudia Rödl,^{1,2} Frank Fuchs,^{1,2} Karsten Hannewald,^{1,2} and Friedhelm Bechstedt^{1,2}

¹*Institut für Festkörperteorie und -optik, Friedrich-Schiller-Universität, Max-Wien-Platz 1, 07743 Jena, Germany*

²*European Theoretical Spectroscopy Facility (ETSF)*

³*Condensed Matter and Materials Division, Lawrence Livermore National Laboratory, Livermore, CA 94550, USA*

Electron doping turns semiconductors conductive even when they have wide fundamental band gaps. The degenerate electron gas in the lowest conduction-band states, e.g. of a transparent conducting oxide, drastically modifies the Coulomb interaction between the electrons and, hence, the optical properties close to the absorption edge. We describe these effects by developing an *ab-initio* technique which captures also the Pauli blocking and the Fermi-edge singularity at the optical absorption onset, that occur in addition to quasiparticle and excitonic effects. We answer the question whether free carriers induce an excitonic Mott transition or trigger the evolution of Wannier-Mott excitons into Mahan excitons. The prototypical *n*-type zinc oxide is studied as an example.

The field of semiconductor optoelectronics is expected to continue its rapid growth in the future, driven, for instance, by the demand for efficient photovoltaics [1] or semiconductor lasers for high-bandwidth optical communication [2]. Degenerate n -doping of a semiconductor introduces a large number of free electrons and, hence, leads to a high conductivity. In particular, the transparent conducting oxides raise hopes for cutting-edge applications [3–5] because they are transparent in the visible spectral range (due to their large fundamental band gaps) and conductive (due to intentional or unintentional n -doping). In these materials, free electrons with a concentration n of up to $\approx 10^{20} \text{ cm}^{-3}$ form a free electron gas in the lowest conduction band (CB) [6, 7]. Even for nominally *undoped* oxides concentrations as large as $\approx 10^{17} \text{ cm}^{-3}$ or even 10^{20} cm^{-3} have been reported [6, 8]. The effect of these free carriers on the optical properties is widely unknown; dramatic changes are expected in the spectral region which is most interesting for applications—the absorption edge.

For undoped semiconductors, experiment [9, 10] and theory [11] consistently describe excitonic states [12] that dominate the absorption below the fundamental band gap. They are caused by the Coulomb attraction between electrons and holes that stabilizes the excited electron-hole pairs. In a degenerately n -doped system a photo-induced electron-hole pair also interacts with the electron gas in the CB via different mechanisms [13, 14]; the screening of the electron-hole attraction is significantly increased by the free carriers. This has been investigated for metals [15], excited semiconductors (Refs. 16 and 17 and references therein), or two-dimensional electron gases in quantum wells [18, 19]. Only recently it is becoming the focus of experimental studies for highly doped semiconductors such as the oxides [7], but also the technologically important nitrides [20] and arsenides [21].

For highly doped semiconductors, the *dissociation* of the excitons, also called excitonic Mott transition [22], has been predicted by theoretical studies of the reduced electron-hole interaction within two-band models based on the effective-mass approximation; however, even though the vanishing of absorption peaks has been observed in experiments, the excitonic Mott transition has never been clearly demonstrated experimentally for bulk semiconductors with a direct band gap. In addition, the filling of the lowest CB states becomes important and it is believed that an excited electron-hole pair which interacts with the Fermi sea still forms a bound state, the so-called *Mahan exciton* [7, 13]. Due to the sharpness of the Fermi surface at low temperatures and Pauli’s exclusion principle, such Mahan excitons cause a singularity of the absorption [13] at the Fermi edge. In a real material, the influence of the temperature and the finite lifetime of photo-generated electron-hole pairs broaden the edge anomalies, which is why these many-body effects cannot be observed easily.

In this Letter, we generalize recent theoretical spectroscopy techniques for the parameter-free calculation of optical properties including excitonic and local-field effects by accounting for an additional degenerate electron gas in the lowest CB: We capture the involved physics, since the CB filling as well as the additional free-carrier contribution to the dielectric screening are included in the calculation of the many-body effects. Our approach is based on the entire quasiparticle (QP) band structure [11] and, hence, includes the non-parabolicity of the bands. Thereby, we go beyond previous models that merely relied on the effective-mass approximation [13, 18, 23]. The present work accomplishes the challenging task of computing all Coulomb-interaction-mediated couplings of electron-hole pairs *consistently* in an *ab-initio* framework. Despite recent efforts [14] such a complete treatment of the free-carrier-modified electron-electron interaction has not been achieved so far. We apply our approach to zinc oxide (ZnO) which is an especially interesting example, since it is abundant in nature, cheap, and biocompatible. Due to a wealth of experimental results, it is an ideal test bed for this work. Moreover, due to the similarity of its band structure to the ones of other transparent conducting oxides, it is of prototypical character. ZnO has a band gap of 3.4 eV [6], a large exciton binding energy of about 60 meV [24], and can easily be n -doped [6].

For several years, *ab-initio* calculations based on many-body perturbation theory are able to describe the QP electronic structure as well as the optical properties of non-metals [11]. In order to treat excitonic and local-field effects, the Bethe-Salpeter equation for the frequency-dependent polarization function P is transformed into an eigenvalue problem for the electron-hole pair Hamiltonian \hat{H} [11]. In the case of partially filled bands the wave-vector dependent occupation numbers $n_v(\mathbf{k})$ and $n_c(\mathbf{k})$ of the Bloch valence band $|v\mathbf{k}\rangle$ and CB $|c\mathbf{k}\rangle$ states take *non-integer* values; we generalize \hat{H} to

$$\begin{aligned} \hat{H}(cv\mathbf{k}, c'v'\mathbf{k}') &= [\varepsilon_c^{\text{QP}}(\mathbf{k}) - \varepsilon_v^{\text{QP}}(\mathbf{k})] \delta_{cc'} \delta_{vv'} \delta_{\mathbf{k}\mathbf{k}'} \\ &+ \sqrt{|n_c(\mathbf{k}) - n_v(\mathbf{k})|} \left[-W(cv\mathbf{k}, c'v'\mathbf{k}') \right. \\ &\left. + 2\bar{v}(cv\mathbf{k}, c'v'\mathbf{k}') \right] \sqrt{|n_{c'}(\mathbf{k}') - n_{v'}(\mathbf{k}')|}. \end{aligned} \quad (1)$$

The first summand in Eq. (1) represents the excitation of *non-interacting* electron-hole pairs with QP energies $\varepsilon_v^{\text{QP}}(\mathbf{k})$, $v = \{v, c\}$. Their *interaction* is described by the statically screened Coulomb attraction of the electron and the hole, $-W$, as well as the unscreened exchange-like term for singlet excitations, $2\bar{v}$, to account for the local-field effects [11]. The optical absorption coefficient $\alpha(\omega)$ is derived from the frequency-dependent macroscopic dielectric tensor $\varepsilon(\omega)$ that is obtained from the solution of the eigenvalue problem for \hat{H} [11].

In Fig. 1a the QP energies and the electron-hole pair interaction around the fundamental gap E_g are illustrated for undoped ZnO [25] at $T = 0 \text{ K}$, i.e., for empty CBs ($n_c(\mathbf{k}) = 0$) and occupied valence bands ($n_v(\mathbf{k}) = 1$). As specified in the following,

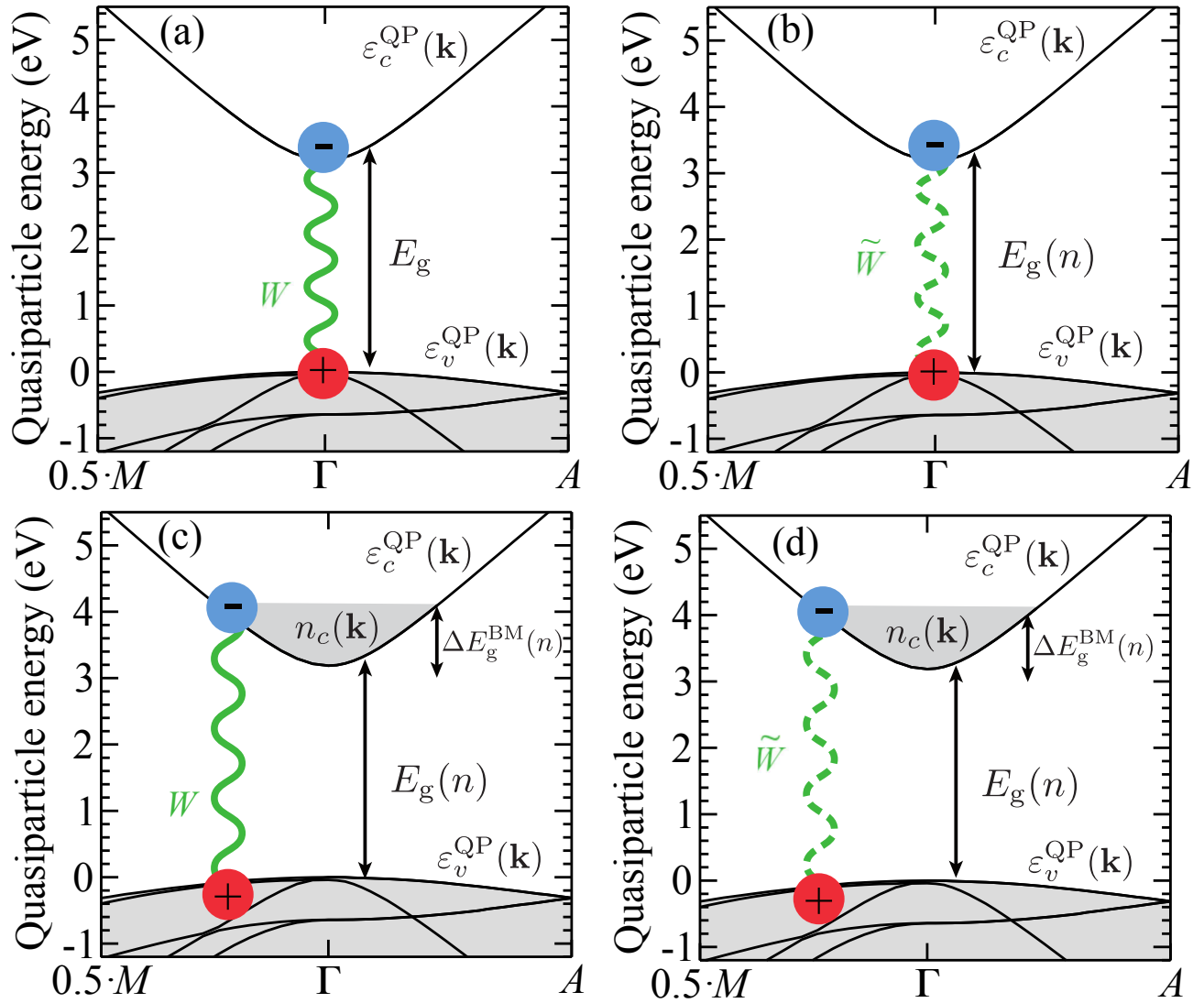


FIG. 1. (Color online) Illustration of free-carrier-induced effects on electron-hole pair excitations near the fundamental band gap of ZnO. (a) Electron-hole interaction (green wavy line) in the undoped material. (b) Additional free-carrier screening affects the electron-hole attraction (dashed green wavy line). (c) Pauli blocking of the lowest CB states causes a Burstein-Moss shift ΔE_g^{BM} of the absorption edge. (d) Both the Pauli blocking as well as the modified screening affect the formation of excitons. The solid lines describe the valence and conduction bands around the fundamental gap.

additional effects on the QP bands, their occupation, and the electron-hole attraction W have to be taken into account when free carriers are present. Up to free-electron densities of about $5 \cdot 10^{21} \text{ cm}^{-3}$, i.e., even for very heavily n -doped ZnO, the occupation of CB states is restricted to the lowest CB c_0 . Summing the occupation number $n_{c_0}(\mathbf{k})$ over the entire Brillouin zone yields the free-electron density, $n = \frac{2}{\Omega_0} \sum_{\mathbf{k}} n_{c_0}(\mathbf{k})$; Ω_0 denotes the volume of the unit cell.

First, the additional carriers cause an intraband contribution to the electronic polarizability [23] which influences the correlation part of the electronic self-energy and, hence, modifies the QP energies $\varepsilon_v^{\text{QP}}(\mathbf{k})$ as well as the screened interaction W . The most important consequence for the QP band structure is the band-gap renormalization (BGR) that leads to $E_g(n) = E_g + \Delta E_g^{\text{BGR}}(n)$ in the doped system [23, 26]. Since the line shape of the absorption coefficient is unaffected by this shift, its discussion is delayed until the results are compared to experiment (cf. Fig. 3).

Second, as illustrated in Fig. 1b and 1d, the electron-hole attraction W is modified due to the electronic intraband polarization caused by the free carriers. Since in (undoped) ZnO the Bohr radius $a_B^{\text{ZnO}} = 1.8 \text{ nm}$ [24] of the lowest excitonic bound state is large compared to the characteristic inter-atomic distances, the small-wave-vector limit is used to describe the free-carrier-induced intraband contribution to the screening. Due to the strong dispersion and the non-parabolicity of the CB, this approximation holds for the doped system in which the free electrons are restricted to a region within 14% of the $\Gamma - M$ distance

at a density of 10^{20} cm^{-3} . Hence, a free-electron-like term $\epsilon_{\text{eff}} \bar{q}_{\text{TF}}^2 / q^2$ for the intraband polarizability is added to the background dielectric constant $\epsilon_{\text{eff}} = 4.4$, where \bar{q}_{TF} denotes the Thomas-Fermi wave vector of free electrons in vacuum. Inside a material \bar{q}_{TF} is modified by the background screening, i.e., $q_{\text{TF}} = \bar{q}_{\text{TF}} / \sqrt{\epsilon_{\text{eff}}}$. Adding this intraband contribution to the screening (cf. Fig. 1b) turns the screened Coulomb potential W in Eq. (1) into a Yukawa-like potential \tilde{W} [27]. This indicates that the degenerate electron gas in the CB reduces the interaction range of the electrons and holes.

Third, the Fermi energy ϵ_{F} lies within the (non-parabolic) CB c_0 when a degenerate electron gas is present. The respective occupation number becomes $n_{c_0}(\mathbf{k}) = \Theta(\epsilon_{\text{F}} - \epsilon_{c_0}^{\text{QP}}(\mathbf{k}))$ in the low-temperature limit. Hence, the lowest CB states around the Γ point in reciprocal space are filled (see Fig. 1c and 1d), which is accounted for by the difference of the occupation numbers in Eq. (1). This so-called Pauli blocking [23] *prevents* optical transitions into these states. For that reason the optical absorption onset occurs at higher energies; this effect is known as Burstein-Moss shift (BMS). Moreover, since the occupation-number factors in Eq. (1) ensure that only electron-hole pairs contribute to the excitonic Hamiltonian, also the influence of the CB filling on the electron-hole interaction (beyond the modified screening) is included.

Electronic-structure calculations are carried out using the Vienna *Ab-Initio* Simulation Package (VASP) [28]. The computational parameters are chosen as described in Ref. 25. Subsequently, these results are used as input to set up the excitonic Hamiltonian (1). In this step, the influence of the doping on the optical absorption is included by taking the modified occupation numbers as well as the influence on the screening into account. Optical absorption into defect-induced electronic states is not captured by this approach. However, in contrast to photoluminescence measurements [29], no indications for such contributions to the optical absorption are found [7] for shallow donors with concentrations up to $4.8 \cdot 10^{19} \text{ cm}^{-3}$. In addition, this approach allows for a very fine sampling of the \mathbf{k} space around the pronounced, non-parabolic CB minimum at the Γ point, hence, [25, 30] free-electron densities as low as $n \approx 10^{17} \text{ cm}^{-3}$ can be resolved. The lowest eigenvalues and eigenstates of the large excitonic Hamiltonian matrix (rank up to $\approx 100,000$) are obtained via iterative diagonalization [30]. The frequency-dependent dielectric function is calculated by means of an efficient time-evolution scheme [31]. To account for finite temperatures and a finite lifetime of the excited electron-hole pairs, as well as a limited instrumental resolution, a Lorentzian broadening of $\gamma = 50 \text{ meV}$ is assumed for the absorption spectra.

As can be seen in Fig. 2 the absorption onset of undoped ZnO is dominated by bound excitonic states. The width and the shape of the peak structure in the absorption spectrum below the fundamental band gap emerge from two underlying exciton series [12, 32], which, however, are not resolved due to the broadening on the order of the exciton binding energy. Even though above E_{g} only scattering states of the excitons occur, the spectrum is still strongly affected by excitonic effects [12, 23]. This is known as Coulomb enhancement.

In order to understand the different effects that arise from the modified electron-hole attraction \tilde{W} and the CB filling, we benefit from performing *ab-initio calculations*, since we investigate these effects separately first, before all free-carrier-induced effects are combined for the comparison to experiment. In a first step, the impact of the free carriers on the screened electron-hole attraction is taken into account ($W \rightarrow \tilde{W}$). The optical-absorption curves in Fig. 2a illustrate that the binding energies and oscillator strengths of the band-edge excitons are reduced due to the smaller interaction range of the electrons and holes. While the absorption edge starts to resemble the one of non-interacting electron-hole pairs, the influence of the additional screening due to the free electrons is small for higher photon energies (cf. Fig. 2a).

The observation that bound excitonic states seem to vanish for high doping levels is interpreted as indication for a Mott transition of the lowest electron-hole pairs. Previous studies (see e.g. Ref. 33 and references therein) investigated a model Hamiltonian consisting of a parabolic kinetic energy term and a Yukawa potential, finding that it has no bound states for inverse screening lengths q_{TF} that fulfill the Mott criterion $q_{\text{TF}} \cdot a_{\text{B}} > 1.19$. Using ϵ_{eff} this relation yields a Mott density of $n_{\text{M}} = 5.94 \cdot 10^{18} \text{ cm}^{-3}$ for which the excitonic Mott transition should occur in ZnO. The spectra in Fig. 2a, calculated for the two free-electron concentrations of $n = 1.9 \cdot 10^{19} \text{ cm}^{-3}$ and $n = 4.8 \cdot 10^{19} \text{ cm}^{-3}$, seem to support this picture, since the pronounced excitonic peak disappears. However, the filling of the CB states has yet been ignored.

Hence, in contrast to Fig. 2a, in Fig. 2b solely the Pauli blocking is taken into account; this shifts the absorption onset towards higher photon energies in n -doped ZnO. More precisely, $\Delta E_{\text{g}}^{\text{BMS}}(n = 1.9 \cdot 10^{19} \text{ cm}^{-3}) = 0.137 \text{ eV}$ and $\Delta E_{\text{g}}^{\text{BMS}}(n = 4.8 \cdot 10^{19} \text{ cm}^{-3}) = 0.236 \text{ eV}$ is derived from the QP band structure. In addition, Fig. 2b indicates that for increasing free-electron concentrations bound excitonic states of \hat{H} persist below the QP band edge (including BMS), i.e. below $E_{\text{g}} + \Delta E_{\text{g}}^{\text{BMS}}(n)$. The artificial increase of the height of the corresponding peaks with increasing n is related to the pronounced Fermi-edge singularity [13] at the absorption onset: when the free-carrier screening is *neglected*, this singularity of the absorption arises from the growing Fermi surface and the modification of the effective electron-hole attraction due to the CB filling [cf. the occupation-number factor in Eq. (1)].

Incorporating the Pauli blocking *and* the additional screening term into the Bethe-Salpeter equation leads to the correct physical description [cf. Eq. (1)]. Hence, the resulting absorption coefficients shown in Fig. 2c can be compared to experiment. The increase of the oscillator strength in Fig. 2b is counteracted by the intraband screening contribution. Comparing Fig. 2c to Fig. 2a reveals that the full approach yields Mahan-exciton-like features [13] at the absorption edge. As shown below in Fig. 3, excitonic bound states still exist; they affect the absorption line shape even when the binding energies are negligibly

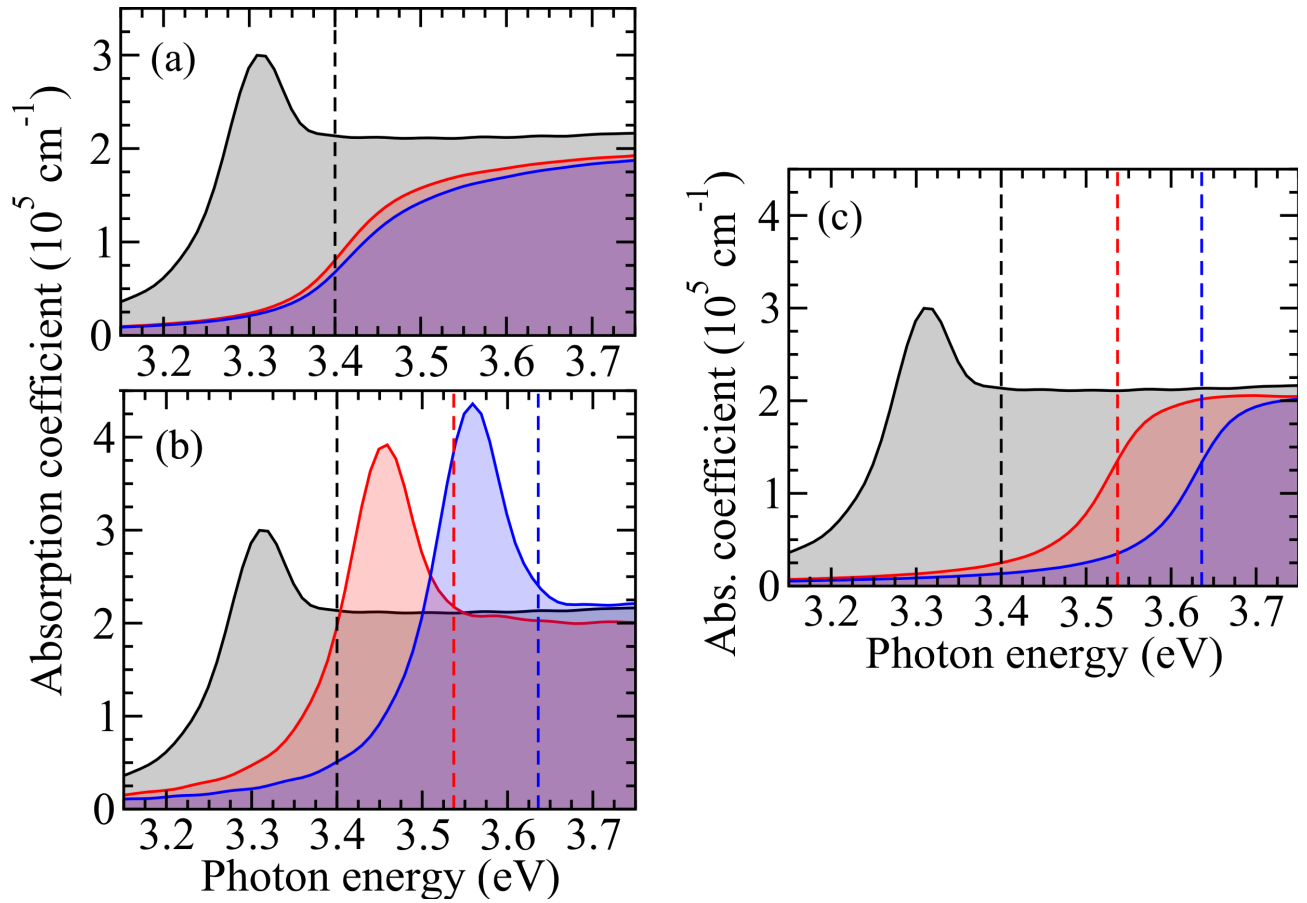


FIG. 2. (Color online) The absorption coefficient of ZnO is plotted versus photon energy for ordinary light polarization. The situation without doping (black curves) is compared to spectra calculated for free-electron concentrations of $n = 1.9 \cdot 10^{19} \text{ cm}^{-3}$ (red) and $n = 4.8 \cdot 10^{19} \text{ cm}^{-3}$ (blue). In (a) the intraband screening due to the free electrons is taken into account. The influence of the Pauli blocking is depicted in (b), and in (c) both effects are included. The respective quasiparticle absorption edges (increased by the Burstein-Moss shift) are indicated by vertical dashed lines.

small. However, due to lifetime, temperature, and instrumental broadening, the Fermi edge and the accompanying singularities are smeared out; hence, in experiment the bound states are not resolved as distinct peaks. The resulting similarity of the curves in Fig. 2a and 2c explains why it is difficult to distinguish between the formation of Mahan excitons and a Mott transition just from the absorption spectra.

In the literature the Mott density is heavily debated; much smaller or much larger values than $n_M = 5.94 \cdot 10^{18} \text{ cm}^{-3}$ have been derived from measured spectra [24]. To enlighten this issue, the binding energy of the lowest excitonic bound state for doped ZnO along with the corresponding oscillator strength is given in Fig. 3a. A rapid decrease of both by orders of magnitude with an increasing density n of the degenerate electron gas is evident. Nevertheless, excitonic states with binding energies of up to 2 meV and oscillator strengths as large as 7% of the value for the lowest bound excitonic state in the undoped material still exist for electron densities *larger* than the nominal Mott density n_M . Hence, no excitonic Mott transition occurs when the full QP band structure, the additional intraband screening, and the Pauli blocking are consistently taken into account. Instead, these states are attributed to Mahan excitons. Mahan found for a two-band model [13] that the binding energy only vanishes for $n \rightarrow \infty$. However, since the decrease is continuous and the influence of broadening effects is large, the behavior depicted in Fig. 3a can readily be mistaken as a Mott transition of the exciton.

The aforementioned *intraband* contribution to the electronic polarizability caused by the additional electrons is small compared to the *interband* screening due to the valence electrons. Hence, its exact treatment within the QP framework is of minor importance. In order to still account for the BGR when comparing the calculated absorption spectra to measured ones, a Lindhard-like description of the intraband polarization is sufficient [26]. The approximate shifts $\Delta E_g^{\text{BGR}}(n = 1.9 \cdot 10^{19} \text{ cm}^{-3}) = -0.213 \text{ eV}$ and $\Delta E_g^{\text{BGR}}(n = 4.8 \cdot 10^{19} \text{ cm}^{-3}) = -0.261 \text{ eV}$ were taken into account for the discussion of the absorption spectra depicted in Fig. 3b.

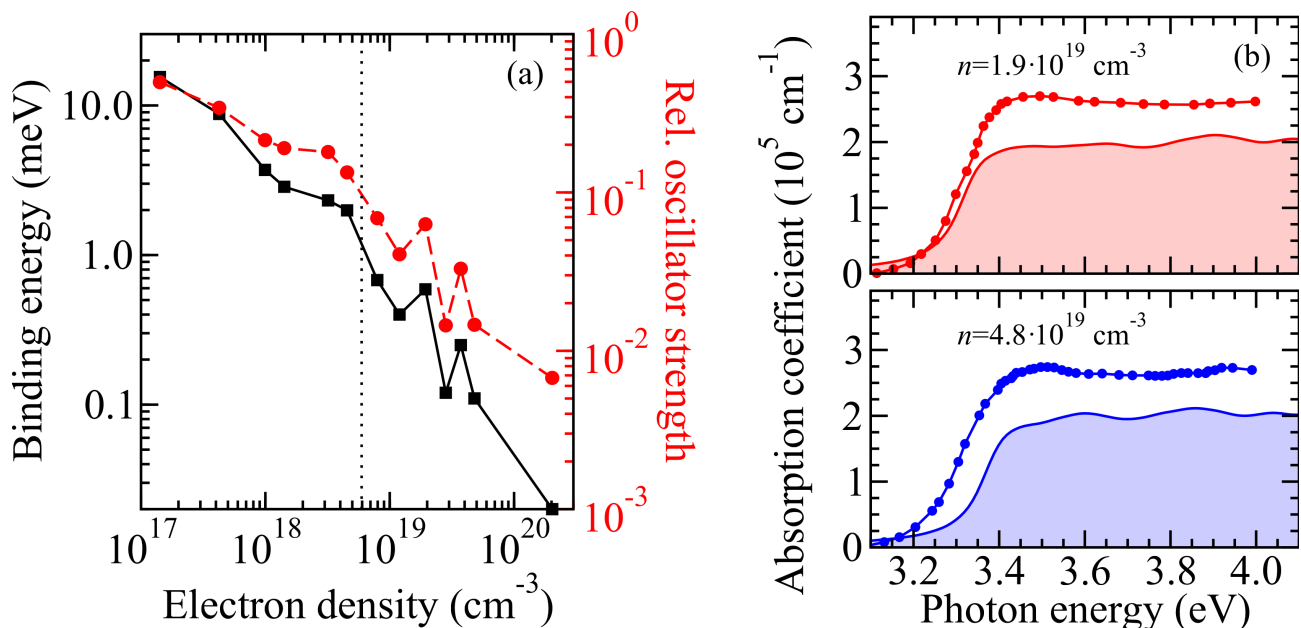


FIG. 3. (Color online) (a) Exciton binding energy (solid) and relative oscillator strength (dashed), normalized with respect to the oscillator strength of the A exciton of undoped ZnO, versus free-electron concentration n . The dotted line indicates the density n_M calculated from the Mott criterion (see text). The fluctuations within $\lesssim 1$ meV arise due to the numerical accuracy. (b) Calculated optical absorption coefficients (solid lines) of n -doped ZnO for ordinary light polarization, with $n = 1.9 \cdot 10^{19} \text{ cm}^{-3}$ (red) or $n = 4.8 \cdot 10^{19} \text{ cm}^{-3}$ (blue). Measured curves (solid lines with dots) are taken from Ref. 7.

Comparing the calculated absorption coefficients to results measured for highly Al-doped ZnO [7] shows very good agreement regarding the energetic position as well as the line shape of the absorption edge (Fig. 3b). The absolute position of the onset and its small variation [7] for different doping levels can be explained by a blueshift (due to the BMS) and a redshift (due to the BGR) that largely compensate each other for $n = 1.9 \cdot 10^{19} \dots 4.8 \cdot 10^{19} \text{ cm}^{-3}$. Having merely used a model [26] to calculate the BGR most likely explains the difference of less than 50 meV between the measured and the calculated position of the absorption onset for $n = 4.8 \cdot 10^{19} \text{ cm}^{-3}$. Overall, Fig. 3b impressively points out that accounting simultaneously for all relevant many-body effects in the calculations yields an unprecedented agreement of the absolute values of the frequency-dependent absorption coefficient with curves measured for doped ZnO. Thereby, any inter-conduction-band absorption is found to be negligible for $n \lesssim 10^{21} \text{ cm}^{-3}$.

In this work, the band-gap renormalization, the Pauli blocking of optical transitions, the reduction of the electron-hole attraction, and the occupation-induced modifications of the electron-hole interaction have been taken into account for a consistent first-principles calculation of the frequency-dependent absorption coefficient of n -ZnO. By disentangling the different many-body effects and their modification caused by the free carriers, we came to a deep, quantitative understanding of the intricate interplay of excitons and doping in transparent conductive oxides. An excellent agreement with experimental results proves that our framework captures the involved physics. Finding no complete dissociation of the lowest bound excitonic state shows that no Mott transition of the exciton occurs; instead, a Mahan-like exciton evolves in the doped system. The approach is readily applicable to other highly doped non-metals and can easily be extended towards p -doped systems.

We acknowledge discussions with P. Rinke, R. Goldhahn, A. Janotti, and C. G. Van de Walle. Financial support by the European Community within the e-I3 project ETSF (GA No. 211956) and the Deutsche Forschungsgemeinschaft (Project No. Be 1346/20-1) is acknowledged. A. S. thanks the Carl-Zeiss-Stiftung and Heptagon for support. Part of this work was performed under the auspices of the U.S. Department of Energy at Lawrence Livermore National Laboratory under Contract DE-AC52-07A27344.

* a.schleife@llnl.gov

- [1] M. Law, L. E. Greene, J. C. Johnson, R. Saykally, and P. Yang, *Nature Materials*, **4**, 455 (2005).
- [2] E. Murphy, *Nat. Photonics*, **4**, 287 (2010).
- [3] Y. Qin, X. Wang, and Z. L. Wang, *Nature*, **451**, 809 (2008).

- [4] E. Comini and G. Sberveglieri, *Mater. Today*, **13**, 36 (2010).
- [5] H. Hosono, in *Handbook of Transparent Conductors*, edited by D. S. Ginley (Springer, 2010) pp. 459–487.
- [6] U. Özgür, Y. I. Alivov, C. Liu, A. Teke, M. A. Reshchikov, S. Doğan, V. Avrutin, S.-J. Cho, and H. Morkoç, *J. Appl. Phys.*, **98**, 041301 (2005).
- [7] T. Makino, K. Tamura, C. H. Chia, Y. Segawa, M. Kawasaki, A. Ohtomo, and H. Koinuma, *Phys. Rev. B*, **65**, 121201 (2002).
- [8] P. H. Jefferson, S. A. Hatfield, T. D. Veal, P. D. C. King, C. F. McConville, J. Zúñiga-Pérez, and V. Muñoz-Sanjosé, *Appl. Phys. Lett.*, **92**, 022101 (2008).
- [9] P. Y. Yu and M. Cardona, *Fundamentals of Semiconductors*, 3rd ed. (Springer, Berlin, 2005) ISBN 3-540-25470-6.
- [10] C. Klingshirn, *Semiconductor Optics* (Springer, Berlin Heidelberg, 2007).
- [11] G. Onida, L. Reining, and A. Rubio, *Rev. Mod. Phys.*, **74**, 601 (2002).
- [12] R. J. Elliott, *Phys. Rev.*, **108**, 1384 (1957).
- [13] G. D. Mahan, *Phys. Rev.*, **153**, 882 (1967).
- [14] M. A. M. Versteegh, T. Kuis, H. T. C. Stoof, and J. I. Dijkhuis, *Phys. Rev. B*, **84**, 035207 (2011).
- [15] M. Combescot and P. Nozières, *J. Phys. France*, **32**, 913 (1971).
- [16] H. Haug and S. Schmitt-Rink, *Prog. Quant. Electron.*, **9**, 3 (1984).
- [17] S. Nojima, *Phys. Rev. B*, **51**, 11124 (1995).
- [18] P. Hawrylak, *Phys. Rev. B*, **44**, 3821 (1991).
- [19] V. Huard, R. T. Cox, K. Saminadayar, A. Arnoult, and S. Tatarenko, *Phys. Rev. Lett.*, **84**, 187 (2000).
- [20] M. Feneberg, J. Däubler, K. Thonke, R. Sauer, P. Schley, and R. Goldhahn, *Phys. Rev. B*, **77**, 245207 (2008).
- [21] F. Fuchs, K. Kheng, P. Koidl, and K. Schwarz, *Phys. Rev. B*, **48**, 7884 (1993).
- [22] N. F. Mott, *Metal-Insulator Transitions* (Taylor & Francis, London, 1990).
- [23] S. Glutsch, *Excitons in Low-Dimensional Semiconductors: Theory, Numerical Methods, Applications* (Springer, 2004).
- [24] C. Klingshirn, R. Hauschild, J. Fallert, and H. Kalt, *Phys. Rev. B*, **75**, 115203 (2007).
- [25] A. Schleife, C. Rödl, F. Fuchs, J. Furthmüller, and F. Bechstedt, *Phys. Rev. B*, **80**, 035112 (2009).
- [26] K. F. Berggren and B. E. Sernelius, *Phys. Rev. B*, **24**, 1971 (1981).
- [27] H. Yukawa, *Proc. Phys. Math. Soc. Jap.*, **17**, 48 (1935).
- [28] G. Kresse and D. Joubert, *Phys. Rev. B*, **59**, 1758 (1999).
- [29] M. Wang, K. E. Lee, S. H. Hahn, E. J. Kim, S. Kim, J. S. Chung, E. W. Shin, and C. Park, *Mater. Lett.*, **61**, 1118 (2007).
- [30] F. Fuchs, C. Rödl, A. Schleife, and F. Bechstedt, *Phys. Rev. B*, **78**, 085103 (2008).
- [31] W. G. Schmidt, S. Glutsch, P. H. Hahn, and F. Bechstedt, *Phys. Rev. B*, **67**, 085307 (2003).
- [32] A. Schleife, C. Rödl, F. Fuchs, J. Furthmüller, and F. Bechstedt, *Appl. Phys. Lett.*, **91**, 241915 (2007).
- [33] Y. Li, X. Luo, and H. Kröger, *Sci. China Ser. G*, **49**, 60 (2006).

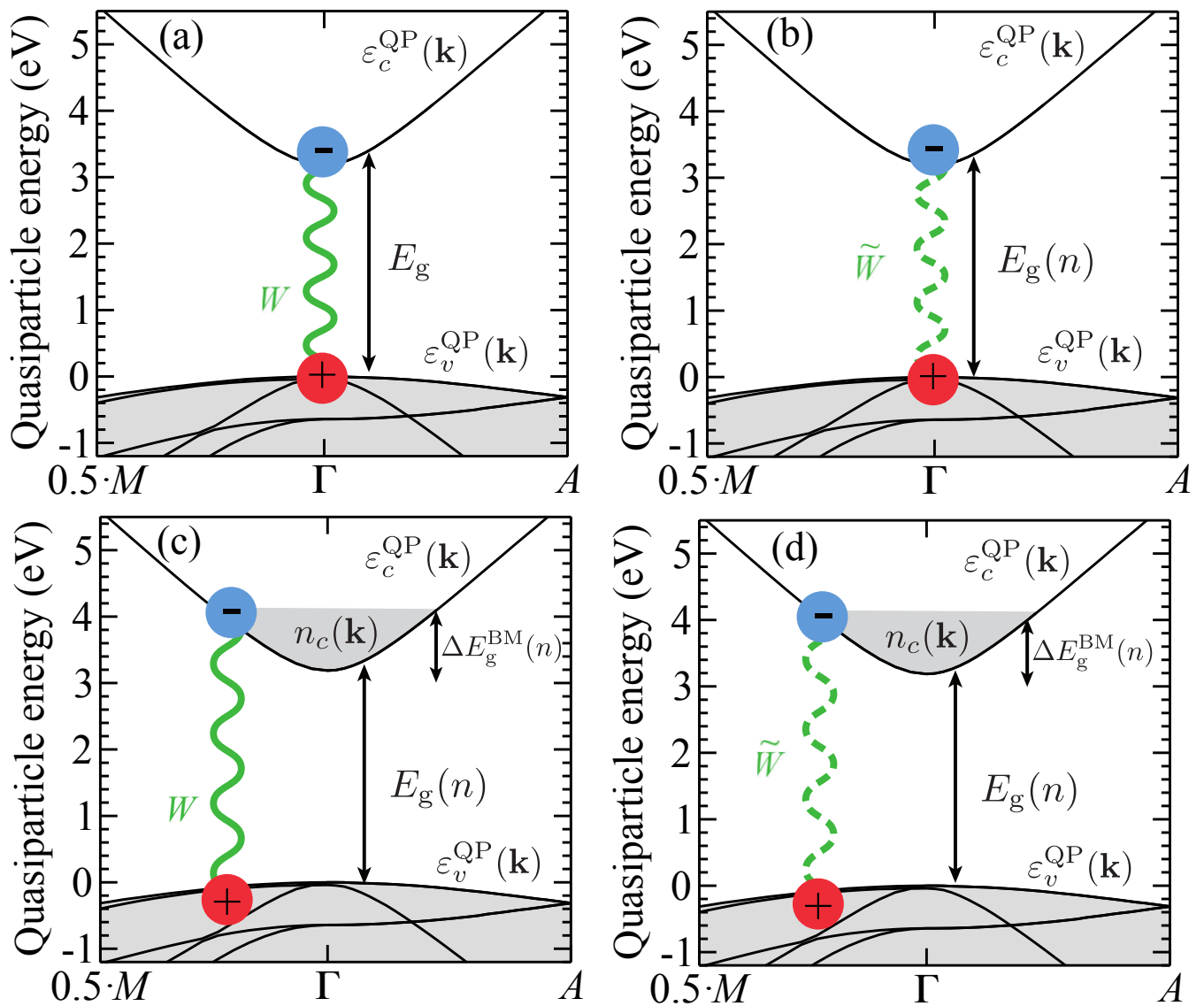


Figure 1 LE13405 20Oct2011

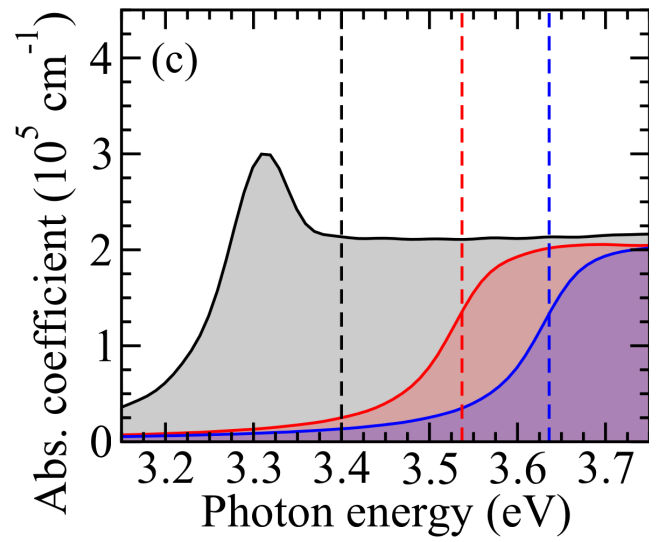
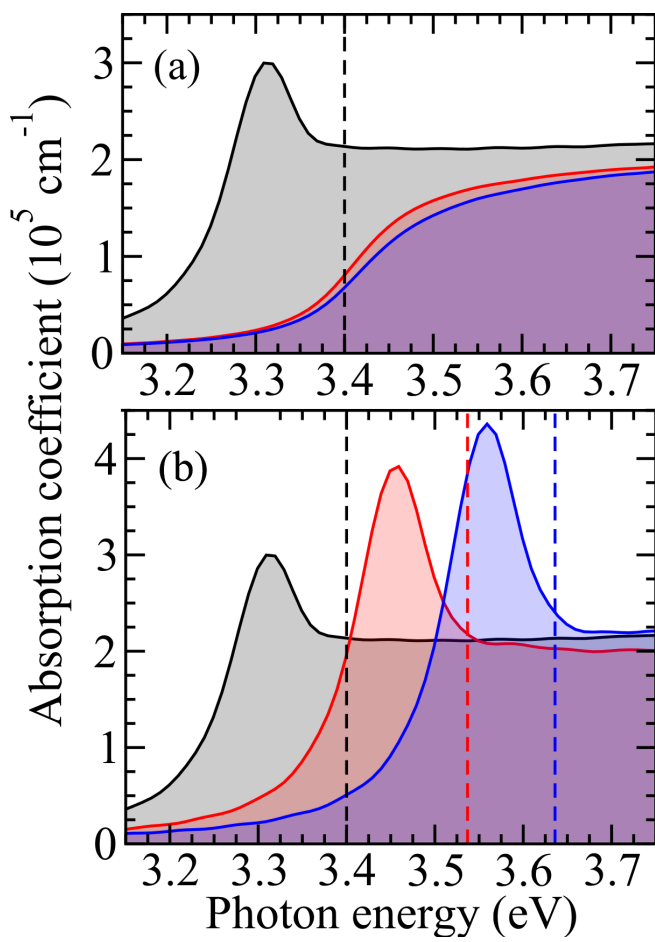


Figure 2

LE13405

20Oct2011

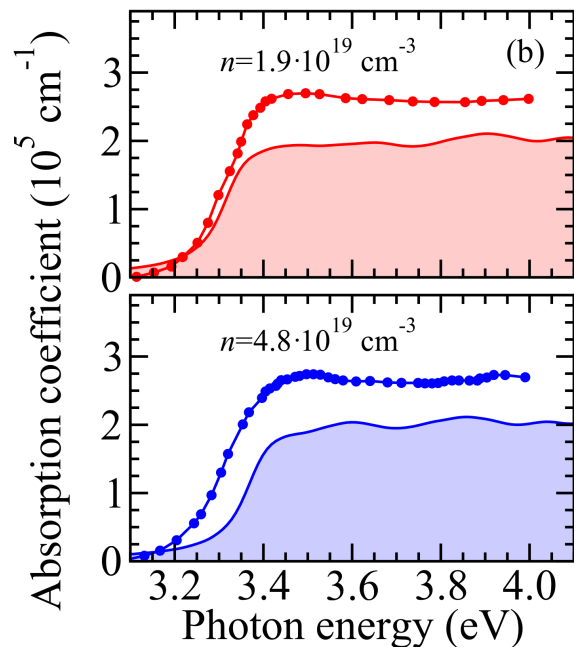
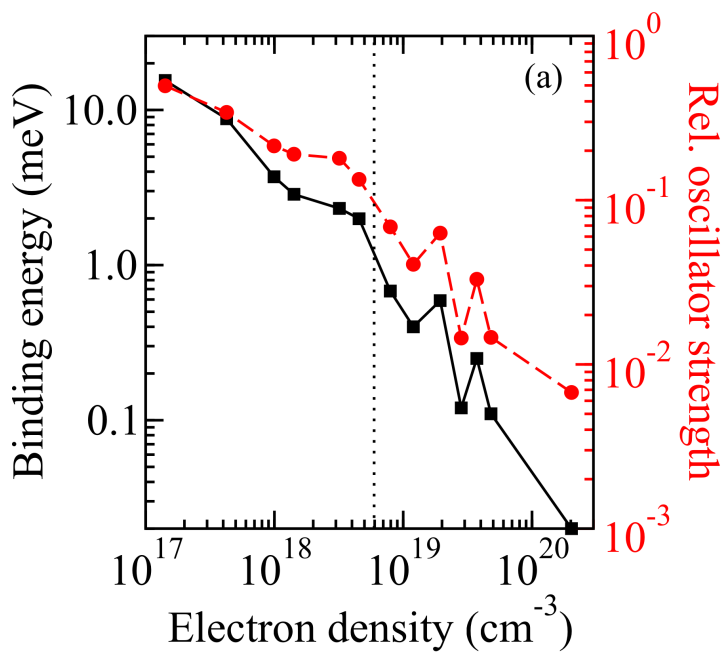


Figure 3 LE13405 20Oct2011